# Investigation on Effect of Flow Direction on Hydrodynamics for Vertical Channel Bubbly Flow

**M. Pang[1]*, J. Wei[2]**

1. School of Mechanical Engineering, Changzhou University, Changzhou, China

2. State Key Laboratory of Multiphase Flow in Power Engineering, Xi'an Jiaotong University, Xi'an, China

**ABSTRACT**

In this paper, the effect of the flow direction on the bubble distribution and the liquid turbulence was deeply investigated with the developed numerical method. The investigated bubbly flow runs in the vertical channel. For the present numerical method, the liquid–phase velocity field was solved by direct numerical simulations and the microbubble trajectories were tracked by Newtonian equations of motion. The present investigations show the flow direction has the key influence on the phase distribution and the liquid–phase turbulence modulation. For the bubbly upflow, the overwhelming majority of microbubbles accumulate near the channel wall, the phase distribution shows approximately the double–peaked distribution pattern, and the liquid–phase turbulence is suppressed. For the bubby downflow, however, microbubbles are far away from the channel wall but move towards the channel centre, the phase distribution shows roughly the off–center–peaked distribution pattern, and the liquid–phase turbulence is enhanced.

## 1. INTRODUCTION

Bubbly flows in pipes or channels are often encountered in power, chemical, food, metallurgy and other industrial fields. Depending on operating conditions, with respect to the normal gravity direction, there are bubbly horizontal flows, bubbly upflows, bubbly downflows and inclined flows. Knowledge of the phase distribution, interactions between bubbles and the liquid–phase turbulent flow are of great importance for designing and operating the bubbly system of industrial applications. Therefore, a great number of studies on hydrodynamic characteristics of bubbly flows have been performed. However, most of the past investigations focused on bubbly upflows in vertical pipes or channels, and quite little attention has been paid to studying bubbly downflows. The related reviews on bubbly upflows can be seen in the references of Lu et al. (2007), Pang et al. (2010) and Lelouvetel et al. (2011).

To our knowledge, recent studies on bubbly downflows were performed by Kashinsky and Randin (1999), Legendre et al. (1999), Hibiki et al. (2004), Sun et al.(2004), Giusti et al. (2005), Kashinsky et al. (2006), Lu and Tryggvason (2006, 2007), Terekhov and

*Corresponding Author: pangmj@cczu.edu.cn

Lelouvetel et al. (2011), and Lelouvetel et al. (2014). Kashinsky and Randin (1999) measured local characteristics of the bubbly downflow such as local void fraction, wall shear stress and velocity fluctuations with an electrochemical technique. Legendre et al. (1999) investigated the radial distribution of bubbles in the pipe upflow and downflow with the numerical method. Hibiki et al. (2004) proposed an approximate radial phase distribution pattern based on experimental data of available references. Sun et al. (2004) analyzed local characteristics of the liquid phase in the air–water downward flow with a laser Doppler anemometry (LDA) system. Giusti et al. (2005) studied microbubble distribution in the upward and downward channel flow with direct numerical simulations without regard for the influence of microbubbles on the liquid–phase turbulence. Kashinsky et al. (2006) studied the local structure of gas–liquid downward flow in a vertical pipe with experimental and numerical methods, respectively. Lu and Tryggvason (2006, 2007) investigated the influence of the relatively large bubbles ($db^+=31.8$) on the liquid–phase turbulence with a low Reynolds number of liquid (Rem=3786). Terekhov and Pakhomov (2008) numerically investigated the effect of bubbles on the turbulence structure and the friction drag in the bubbly downflow. Lelouvetel et al. (2011) investigates the turbulence modifications by bubbles in a bubbly downflow with a time–resolved particle tracking velocimetry (PTV) system. Lelouvetel et al. (2014) analyzed the turbulent energy cascade in a bubbly pipe downflow with an experimental method.

As a matter of fact, although many studies on bubbly upward or downward flows in the vertical pipes or channels have been performed, mechanisms on the liquid–phase turbulence modulation by bubbles are not fully understood yet. Especially, understandings of the liquid–phase turbulence modulation by bubbles in vertical downward pipe or channel flows are very limited. Due to current energy shortage, a fashionable application for bubbly flows is turbulence drag reduction by the microbubble injection. Depending on operating conditions, bubbly flows may show various flow directions in an actual industrial environment. Therefore, it is very necessary for designing the drag–reducing system by microbubbles to deeply understand the influence of the flow direction on the liquid–phase turbulence modulation.

In this paper, the bubbly flow laden with microbubbles runs upward and downward in the vertical channel, respectively. For two kinds of flows, the phase distribution and the liquid–phase turbulence were in detail investigated with the developed Euler–Lagrange two–way model. For the present computation, microbubbles were considered to be fully contaminated, and thus their behavior is just like a small rigid sphere. Besides, to simplify the present computation and reduce the computational load, the global void fraction ($\alpha_0=1.34\times10^{-4}$) was very low so that interactions among microbubbles can be neglected.

## 2 COMPUTATIONAL CONDITION AND GOVERNING EQUATIONS

### 2.1 Computational condition

The vertical channel bubbly upward and downward flows laden with microbubbles were simulated. The computational domain size is $10h\times2h\times5h$ corresponding to the streamwise (x), wall-normal (y) and spanwise (z) direction, respectively. Here, h is the channel half width. Gravity is exerted on the negative x direction (for the upward flow) and on the positive x direction (for the downward flow). The effect of gravity on the bubbly flow was reflected by the Froude number ($Fr=0.0169$) in the governing equations. Periodic boundaries were applied to both the streamwise and spanwise direction for liquid and

microbubble phases. In the wall-normal direction, however, no-slip boundaries were exerted on the channel walls for the liquid phase and the wall elastic collision reflection condition excluding energy loss was used for microbubbles. The shear Reynolds number of the liquid phase was $Re_\tau = 150$, which was based on channel half width (h) and wall friction velocity ($u_\tau = (\tau_w/\rho_f)^{1/2}$). Where $\tau_w$ is the statistically averaged wall shear stress and $\rho_f$ is the liquid density. The liquid phase was considered to be incompressible, isothermal and with constant properties, and its thermophysical property data were used as those of water at room temperature, $\rho_f = 1000\ kg/m^3$. The microbubbles were regarded to be spherical in shape, and their density is $\rho_b = 1.3\ kg/m^3$. The microbubble diameter is $d_b = 0.011h$, and the global void fraction is $\alpha_0 = 1.34 \times 10^{-4}$. When a statistically steady state of the liquid-phase turbulence was reached, a swarm of microbubbles were randomly seeded into the liquid-phase turbulence for the same flow. The initial velocity of microbubbles was set to zero. For the present investigation, the effect of microbubbles on the liquid density was negligible since the global void fraction is very low. Accordingly, the effect of ″density effect″ on the liquid turbulence modulation can be neglected.

## 2.2 Governing equations

To investigate numerically the channel bubbly flow laden with microbubbles, an Eulerian–Lagrangian method was successfully developed by Pang et al. (2010). For the developed numerical method, the liquid–phase continuity and momentum equations were solved in an Eulerian framework, while the microbubble trajectories were tracked by motion equations following to Newton′s second law. The coupling between microbubble and liquid phases was accomplished by regarding the sum of all interphase forces as a source term of the liquid–phase momentum equation.

Allowing for that non-dimensional variables have the universal meaning, all of them are normalizated. The parameters related to length scale are normalizated by half the channel width ($h$), parameters having something to do with velocity scale are normalizated by the friction velocity ($u_\tau$), and variables related to time scale are normalizated by $h/u_\tau$. In the governing equations, the non-dimensional values of velocity, length, pressure, time and interfacial force are defined as follows, respectively.

$$u_i^+ = \frac{u_i}{u_\tau},\quad x_i^* = \frac{x_i}{h},\quad p^+ = \frac{p}{\rho_f u_\tau^2} = p^{+*} - x^*,\quad t^* = \frac{t}{h/u_\tau},\quad f_i^* = \frac{F_i}{u_\tau^2/h}.$$

Here, the pressure is decomposed into the fluctuating pressure $p^{+*}$ and the average value $-x^*$ driving the mean flow. The definitely normalizated process on the governing equations can be referred to the literature (Pang et al., 2010). The non-dimensional governing equations for the liquid phase can be written as follows.

Dimensionless continuity equation:

$$\frac{\partial u_{fi}^+}{\partial x_i^*} = 0 \tag{1}$$

Dimensionless momentum equation:

$$\delta_{max} = \frac{\partial u_{fi}^{+}}{\partial t^{*}} + u_{fj}^{+}\frac{\partial u_{fi}^{+}}{\partial x_{j}^{*}} = -\frac{\partial p^{+*}}{\partial x_{i}^{*}} + \delta_{Ii} + \frac{1}{Re_{\tau}}\nabla^{2}u_{fi}^{+} - f_{i}^{*} \tag{2}$$

The non-dimensional governing equations for the bubble phase can be written as following:

$$\underbrace{\frac{\rho_b}{\rho_f}\frac{du_{bi}^{+}}{dt^{*}}}_{inertia\ \ force} = \underbrace{\frac{Du_{fi}^{+}}{Dt^{*}}}_{pressure\ gradient\ \ force} + \underbrace{\frac{3}{4}\frac{C_D}{d_b^{*}}\left|u_{fi}^{+}-u_{bi}^{+}\right|\left(u_{fi}^{+}-u_{bi}^{+}\right)}_{drag\ \ force} + \underbrace{C_v\left(\frac{Du_{fi}^{+}}{Dt^{*}}-\frac{du_{bi}^{+}}{dt^{*}}\right)}_{added\ \ mass\ \ force} + \underbrace{C_{LF}\varepsilon_{ijk}\varepsilon_{klm}\left(u_{fi}^{+}-u_{bi}^{+}\right)\frac{\partial u_{fl}^{+}}{\partial x_{m}^{*}}}_{shear\ \ lift\ \ force} + \underbrace{\left(1-\frac{\rho_b}{\rho_f}\right)\frac{1}{Fr^{2}}}_{gravity}$$
$$+ \underbrace{\delta_{2i}\left|u_{fi}^{+}-u_{bi}^{+}\right|^{2}\max\left(0,-\frac{0.0064}{d_b^{*}}+\frac{0.016}{y^{*}}\right)}_{wall\ \ lift\ \ force} \tag{3}$$

Where $u_i^{+}$ is the velocity in the ith direction, $p^{+*}$ is the transient pressure, $\rho$ is the density, $\delta_{ij}$ is Kronecker Delta denoting the mean pressure, $\varepsilon$ is sign of permutation, $t^{*}$ is the time, and $x_i^{*}$ is the coordinate variable. Subscripts $b$ and $f$ denote the microbubble and liquid phase, respectively. In Eqn. (2), $\overline{f_i^{*}}$ denotes the feedback force exerted on the liquid phase by microbubbles, which denotes the effect of microbubbles on the liquid turbulence. The detailed computation on the feedback force can be seen in the reference (Pang et al., 2010). In Eqn. (3), $C_D$ is the drag coefficient, $C_v$ is the added mass coefficient ($C_v$=*0.5*), $C_{LF}$ is the lift coefficient, and $Fr$ is the Froude number ($F_r = \frac{u_\tau}{\sqrt{gh}}$), $g$ is the gravitational acceleration). The drag coefficient is calculated by the following empirical correlation (Laín et al., 2002):

$$C_D = \begin{cases} \dfrac{16}{\mathrm{Re_b}} & \mathrm{Re_b} \le 1.5 \\ \dfrac{14.9}{\mathrm{Re_b}^{0.78}} & 1.5 \le \mathrm{Re_b} < 80 \\ \dfrac{48}{\mathrm{Re_b}}\left(1-\dfrac{2.21}{\sqrt{\mathrm{Re_b}}}\right)+1.86\times10^{-15}\,\mathrm{Re_b}^{4.756} & 80 \le \mathrm{Re_b} < 1500 \\ 2.61 & 1500 \le \mathrm{Re_b} \end{cases} \tag{4}$$

The lift coefficient is computed by the correlation proposed by Legendre and Magnaudet (1998):

$$C_{LF} = \sqrt{\left\{C_L^{\text{low Re}}\left(\mathrm{Re_b},\mathrm{Sr_b}\right)\right\}^{2} + \left\{C_L^{\text{high Re}}\left(\mathrm{Re_b}\right)\right\}^{2}} \tag{5}$$

where

$$C_L^{\text{low Re}}\left(\mathrm{Re_b},\mathrm{Sr_b}\right) = \frac{6}{\pi^{2}}\left(\mathrm{Re_b}\cdot\mathrm{Sr_b}\right)^{-0.5}\left[\frac{2.255}{\left(1+0.2\zeta^{-2}\right)^{1.5}}\right],\ C_L^{\text{high Re}}\left(\mathrm{Re_b}\right) = \frac{1}{2}\left(\frac{1+16/\mathrm{Re_b}}{1+29/\mathrm{Re_b}}\right).$$

Where $Sr_b$, $Re_b$ are the dimensionless shear rate ($Sr_b = |\omega_b| \frac{d_b}{2} |u_f - u_b|$) and the bubbles Reynolds number ($Re_b = \frac{|u_f - u_b| d_b}{\nu_f}$), respectively, and $\zeta = \sqrt{\frac{Sr_b}{Re_b}}$.

## 3 NUMERICAL METHODS

The governing equations for liquid flow were discretized with a finite difference scheme based on the staggered grid. Velocity components in three directions were stored at the face center of the grid, and the pressure was stored at the center of the grid. A second–order finite difference scheme was applied to the spatial discretization. For the time integration, the second–order Adams–Bashforth scheme was used for all the terms except the implicit method for the pressure term. To calculate the interphase force related to the relative velocity between the microbubble and the local liquid, the three–dimensional 8–node combined with the two–dimensional 4–node interpolation polynomials were used to calculate the liquid velocity at the same position of the microbubble (near the wall, the interpolation scheme switches to one side). The motion equations of microbubbles were solved in time with the second–order Crank–Nicholson scheme to compute the velocities and displacements of microbubbles. The detailed numerical methods on single– and two–phase flow were described in the literature (Pang et al., 2010).

For the present simulation, the grid system was absolutely same to that developed in the reference (Pang et al., 2010). Authors had verified that the grid system can be applied to simulate the bubbly flow. The grid resolution was 64×64×64 in each direction. The computational grid was equispaced in the streamwise and spanwise direction, and the non–uniform grids were used in the wall–normal direction with the denser mesh near the channel walls. The grid spacing was $\Delta x^+=23.4$ and $\Delta z^+=11.7$ in the streamwise and spanwise direction, respectively. In the wall–normal direction, the grid space $\Delta y^+$ varied from 0.45 close to the wall to about 9 near the channel centre. The present grid resolution was verified to meet the needs of the liquid-phase direct numerical simulations too, and its details see the reference of Pang et al. (2010). Additionally, the length unit "$^+$" is based on "wall units", and it is normalizated by viscous length scale ($\frac{\nu_f}{u_\tau}$), such as $y^+ = \frac{y u_\tau}{\nu_f}$. Here, $\nu_f$ and $u_\tau$ denote the kinematic viscosity and the fiction velocity of the bubble-free liquid flow, respectively.

## 4 RESULTS AND DISCUSSION

### 4.1 The phase distribution

As pointed out by Legendre et al. (1999), the phase distribution has the significant effect on the momentum, heat and mass transfer between bubble and liquid phases so it is very important to understand the lateral distribution of microbubbles in the channel or pipe. Here, Fig. 1 firstly shows the local void fraction profile for the bubbly upflow and downflow laden with microbubbles. In Fig.1, the horizontal ordinate ($y^+$) is the wall coordinate system. It can be seen from Fig. 1 that, for the bubbly upflow, the local void fraction displays the approximate double–peaked profile pattern. One big peak appears in the location very closer to the channel wall, and the other small one occurs in the location near the buffer-layer brim. Different form the bubbly upflow, however, for the bubbly downflow, the local void fraction shows the approximate off–center–peaked distribution pattern by the definition of Hibiki et al. (2004). Namely, a very weak peak appears in the location far away from the channel central region, and the local void fraction has a finite value in the region very closer to the

channel wall. As far as the bubbly upflow and downflow is concerned, the biggest difference shows that the sign of the relative velocity between bubbles and liquid is opposite. For the bubbly upflow, the relative velocity between them is positive. It means that the shear lift force always points to the channel wall so as to drive microbubbles to move towards to the channel wall. For the bubbly downflow, however, the relative velocity is negative, which changes the shear lift force direction. Thus, the shear lift force always points to the channel centre and brings microbubble away from the channel wall. Therefore, the local void fraction shows different distribution pattern for different flow direction.

For the channel turbulence, the vortex activity is relatively frequent in the buffer layer, so the liquid–phase pressure is relatively lower in the region near the buffer layer than in other regions. If the pressure on the left and right sides of the microbubble is unequal, the pressure gradient force will drive microbubbles to move from the high pressure region to the low pressure one. For the present investigation, the appearance of the relatively small peak for the bubbly upflow and the very weak peak for the bubbly downflow may be just caused by the pressure gradient force. Whether for the bubbly upflow or for the bubbly downflow, if microbubbles want to leave the low–pressure region to approach the channel wall for the upflow (or to move towards the channel centre for the downflow), they have to overcome the resistance of the pressure gradient force.

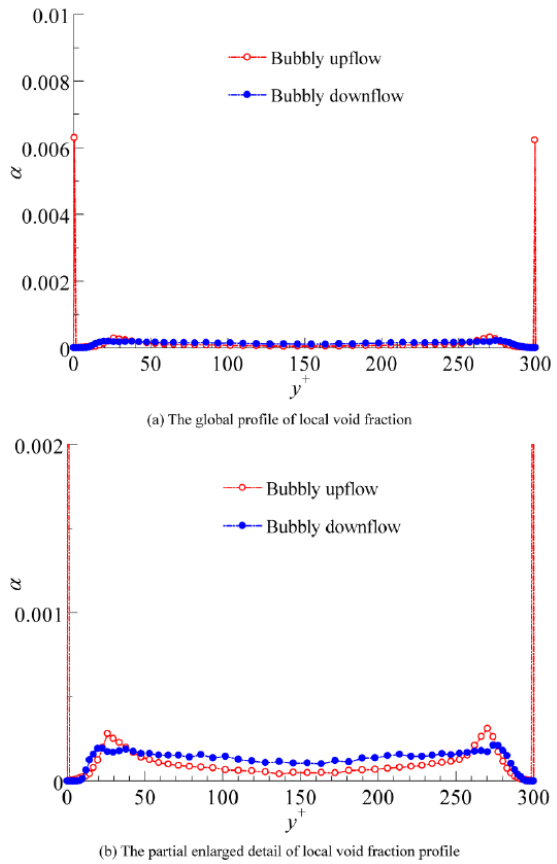


Figure 1: Local void fraction profile.

### 4.2 The liquid–phase turbulence modulation

It is very important for designing and operating the bubbly system (especially the drag–reducing system by microbubbles) to fully understand the liquid–phase turbulence modulation by microbubbles. The modulation of microbubbles on the liquid–phase turbulence is reflected through analyzing the effect of microbubbles on the liquid–phase turbulence statistics. Fig. 2 shows the mean streamwise velocity profiles of the microbubble and liquid phase. For comparisons, Fig. 2(a) also shows the classical law–of–the–wall velocity profile of Newtonian fluid (including the linear law in the viscous sub–layer and the logarithmic law in the outer layer). It can be seen that the mean streamwise velocity of the single liquid phase is in good agreement with the classical law–of–wall velocity profile of Newtonian fluid, showing that the present computation is credible. Compared with the single liquid phase, the addition of microbubbles increases the mean streamwise velocity of the liquid phase for the bubbly upflow but it decreases that for the bubbly downflow. Under the action of the same pressure gradient, the increase of the mean velocity of the liquid phase means the decrease of turbulence friction drag for the bubbly upflow, however, the contrary thing occurs to the bubbly downflow. Namely, for the bubbly downflow, the microbubbles injection decreases the mean velocity of the liquid phase but increases the turbulence frictional drag. For the bubbly downflow, the present computational results are similar to computational ones of Lu and Tryggvason (2006, 2007) and experimental ones of Terekhov and Pakhomov (2008).

The influence of microbubbles on the liquid–phase velocity cannot be simply ascribed to the pull effect of buoyance, as analyzed in previous studies of authors (Pang et al., 2011). As a matter of fact, as shown in Fig. 2(b), the microbubbles flow faster than liquid for the upflow but they flow more slowly than liquid for the downflow under the influence of buoyance. The relative velocity between the microbubble and liquid leads to the occurrence of the interphase drag force. For the bubbly upflow, the drag force will pull the liquid phase to accelerate, which may cause the increase of the liquid–phase velocity. Inversely, for the bubbly downflow, the drag force will cause the liquid phase to decelerate, which may lead to the decrease of the liquid–phase velocity. In our opinion, the pull effect of buoyance is one of reasons changing the liquid–phase velocity but it is not the only one. The influence of microbubbles on the liquid–phase turbulence is very complex. Especially, the liquid–phase turbulence modulation by microbubbles is bound to change the liquid–phase velocity. Accordingly, it is very necessary to analyze the effect of microbubbles on the high–order turbulence statistics in detail.

Figure 3 show the liquid–phase velocity fluctuation intensity profile. It can be seen from Fig. 3 that the influence of microbubbles on the liquid–phase velocity fluctuation intensity is totally different for the bubbly upflow and downflow. Whether for the bubbly upflow or for the bubbly downflow, the influence of microbubbles on the streamwise component is more complex than that on the wall–normal and spanwise components. Namely, the addition of microbubbles causes different effect on the streamwise component corresponding to different wall–normal locations. For the bubbly upflow, the microbubbles injection has no influence on the streamwise component in the region of $0<y^+<5$, increases it in the region of $5<y^+<50$ and decreases it in the region of $50<y^+<150$. And it totally decreases the wall–normal and spanwise components in the channel width region. However, the opposite things happen to the bubbly downflow for the velocity fluctuation intensity of the liquid phase. The decrease (increase) of the liquid–phase velocity fluctuation intensity for the bubbly

upflow (for the bubbly downflow) means the decrease (increase) of energy consumed by the velocity fluctuation. The saved (dissipated) energy for the upflow (for the downflow) may be applied to accelerate (decelerate) liquid, as shown in Fig. 2(a). Accordingly, the change of the liquid–phase mean velocity may be directly related to the liquid–phase turbulence modulation by microbubbles.

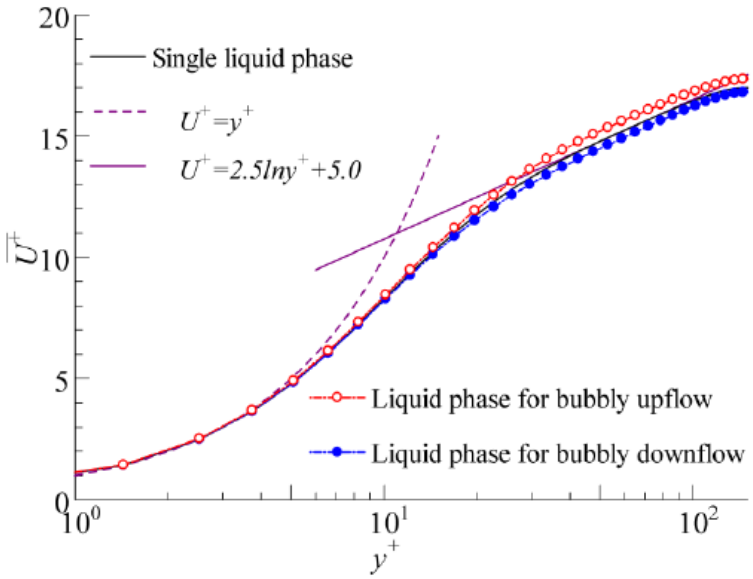


(a) Liquid phase

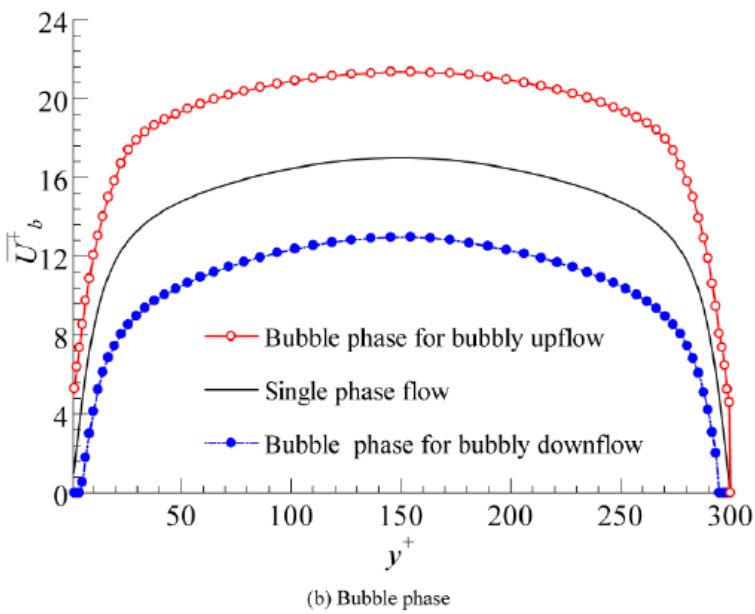


(b) Bubble phase

Figure 2: Mean streamwise velocity profile of liquid and bubble phase

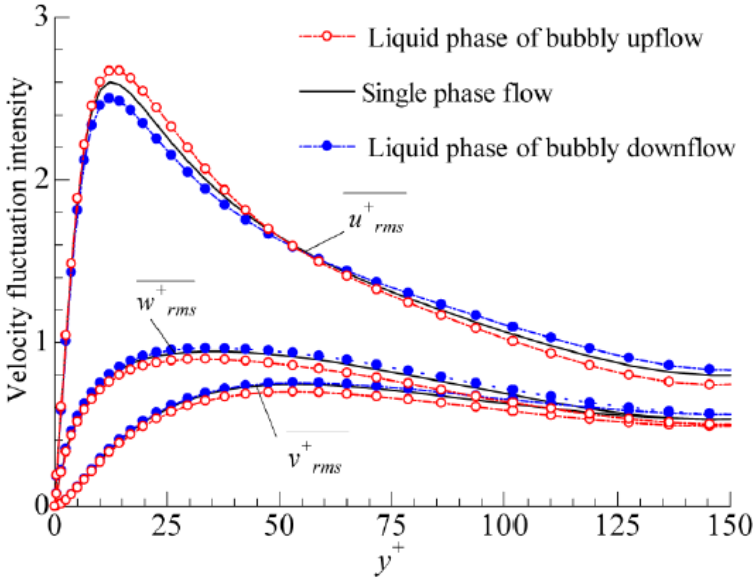


Figure 3: Velocity fluctuation intensity profile of liquid

The modification of microbubbles on the liquid–phase velocity fluctuation intensity is very complicated. Up to now, there is not a fully acceptable mechanism explanation on this physical phenomenon. In this paper, one mechanism explanation on the liquid–phase turbulence modulation by microbubbles is shown in Fig. 4. Ortiz–Villafuerte and Hassan (2006) pointed out that the effect of microbubbles on the turbulence fiction drag is mainly determined by the void fraction value in the buffer layer. The present computation shows that the local void fraction has a weak peak in the buffer layer ($y^+\approx 20$) for both the bubbly upflow and downflow as shown in Fig. 1(b), respectively. The location of $y^+\approx 20$ can be approximately considered to be the division point between the low–velocity and high–velocity regions. In the region of $y^+<20$, the mean streamwise velocity changes sharply, and the velocity gradient is great; only a small disturbance may cause the big change of the velocity fluctuation intensity. For the bubbly upflow, the shear lift force on the microbubble always points to the channel wall. Under the influence of the shear lift force, the microbubbles move from the centre to the wall of the channel. Thus, the low–velocity liquid is difficult to leave the low–velocity region to the high–velocity one under the resistance of microbubbles. However, the high–velocity liquid can move from the high–velocity region to the low–velocity one under the drive of microbubbles. Accordingly, the streamwise velocity fluctuation decreases in the region of $50<y^+<150$ because the microbubbles hinder the low–velocity liquid to leave the low–velocity region (i.e., stop the momentum transfer between the high–velocity and low–velocity liquid); it increases in the region of $5<y^+<50$ because the microbubbles enhance the high–velocity liquid to move toward the low–velocity region (namely, enhance the momentum transfer between the low–velocity and high–velocity liquid); and it almost keeps unchanged in the region of $0<y^+<5$ because the high–velocity liquid is very difficult to approach this region due to the resistance of the strong eddy motions in the buffer layer.

However, for the bubbly downflow, the shear lift force on the microbubble is directed at

the channel centre. Under the action of the shear lift force, the microbubbles are away from the channel wall and move towards the channel centre. When the microbubbles move towards the channel centre, they may hinder the movement of the high–velocity liquid towards the low–velocity region but may promote the movement of the low–velocity liquid towards the high–velocity region. The above phenomena may reduce the momentum transfer in the low–velocity region and may enhance that in the high–velocity region. Accordingly, the streamwise component of velocity fluctuation intensity decreases in the region of $5<y^+<50$ and increases in the region of $50<y^+<150$. Additionally, when the computation reaches the statistical steady state, there are not microbubbles in the region of $0<y^+<5$; therefore, the streamwise component of velocity fluctuation intensity almost keeps unchanged in this region.

The influence of microbubbles on the lateral components of velocity fluctuation intensity can be explained as follows. For the bubbly upflow, the migration of microbubbles towards the channel wall may prevent the development of vortexes near the wall towards the high–velocity region, which reduces the lateral components of velocity fluctuation intensity. However, for the bubbly downflow, the movement of microbubbles away from the channel wall and towards the channel centre may promote the development of vortexes towards the high–velocity region, so it increases the lateral components of velocity fluctuation intensity. As a matter of fact, the liquid–phase velocity fluctuation has the direct relation to the eddy motions with different scales. In short, the present analyses show that the shear lift force is a very important factor for the liquid–phase turbulence modification. That is in good agreement with conclusions of Giusti et al. (2005).

In order to further analyze the effect of microbubbles on the liquid–phase turbulence, Figure 4 shows the streamwise and spanwise components of vortex fluctuation intensity of liquid. One can see from Figs. 3 and 4 that the effect of microbubbles on the streamwise component of velocity and vortex fluctuation intensity is somewhat similar. Compared with the single liquid phase, for the bubbly upflow, the streamwise component of vortex fluctuation intensity almost keeps unchanged in the region of $0<y^+<5$, and it increases in the region of $5<y^+<35$ and decreases in the region of $35<y^+<150$. For the bubbly downflow, however, it also almost keeps unchanged in the region of $0<y^+<5$, slightly decreases in the region of $5<y^+<35$ and increases in the region of $35<y^+<150$. It can be also seen from Figs 3 and 4 that the effect of microbubbles on the spanwise component of velocity and vortex fluctuation intensity is totally different. For the bubbly upflow, the spanwise component of vortex fluctuation intensity somewhat increases near the wall and slightly decreases in the region away from the wall. However, the opposite things happen to the spanwise component for the bubbly downflow. As described above, for the bubbly upflow, when the microbubbles move towards the channel wall, they will prevent the high–frequency and small–scale spanwise vortexes in the buffer layer from developing towards the channel centre. And the microbubble accumulation near the channel wall may weaken energy transfer and scale transformation between the small–scale vortexes near the channel wall and the big–scale ones in the channel centre. However, for the bubbly downflow, the microbubbles leave the wall to the channel centre, meanwhile, they will drive the high–frequency and small–scale spanwise vortexes in the buffer layer to develop towards the channel centre. That fact will enhance the energy transfer and scale transformation between the small–scale vortexes near the channel wall and the big–scale ones in the channel centre. Furthermore, for the bubbly upflow, the addition of microbubbles reduces the energy transfer from the large–scale eddies (denoting the mean flow) to the small–scale eddies

(denoting energy dissipation) so the liquid–phase turbulence fluctuation decreases but the mean streamwise velocity increases. However, for the bubbly downflow, it enhances the energy transfer between both of them so the liquid–phase turbulence fluctuation increases but the mean streamwise velocity decreases.

Figure 6 shows the instantaneous spanwise vortex contour. It can be seen from Fig. 6 that the positive and negative spanwise vortexes occur in turn near the channel wall. Compared with the single liquid phase, the spanwise vortex seems to be relatively denser and stronger near the wall for the bubbly upflow, however, it seems to be relatively diluter and weaker near the wall and develops more obviously outwards for the bubbly downflow. Those phenomena are in agreement with the above inferences.

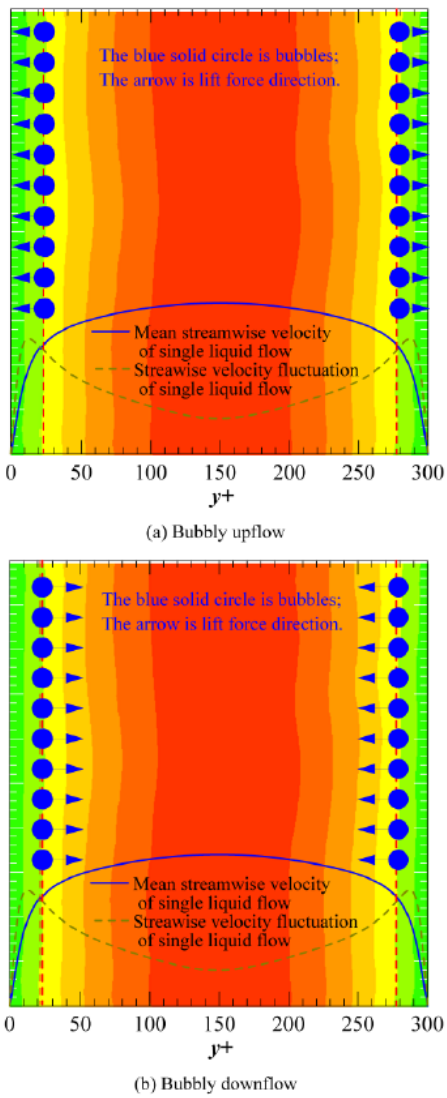


Figure 4: Influences of bubbles on liquid-phase turbulence model.

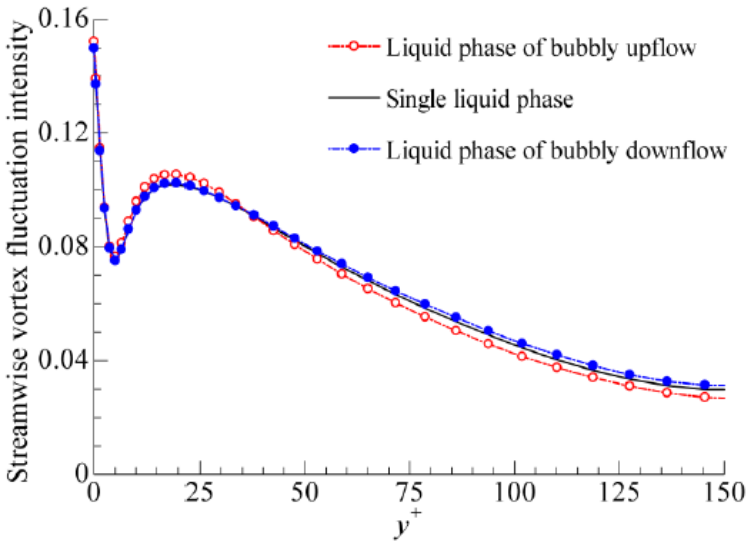


(a) The streamwise component

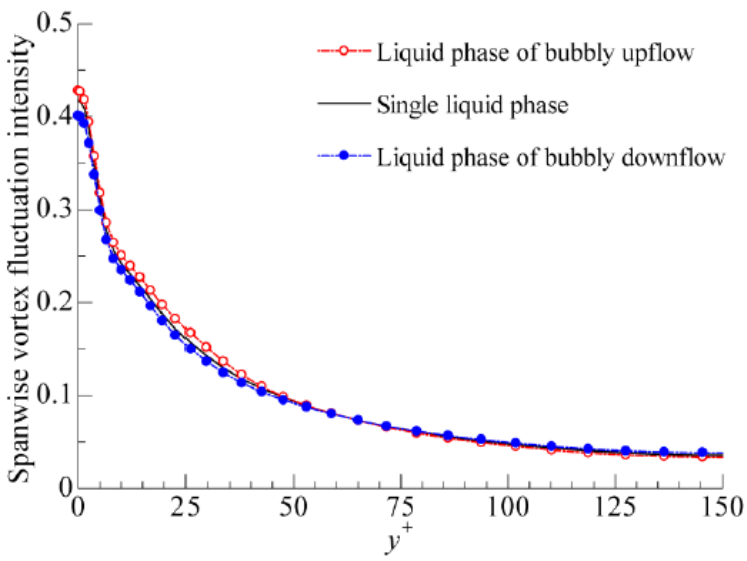


(b) The spanwise component

Figure 5: Vortex fluctuation intensity profile of liquid.

In order to further analyze the effect of microbubbles on the liquid–phase turbulence, Figure 4 shows the streamwise and spanwise components of vortex fluctuation intensity of liquid. One can see from Figs. 3 and 4 that the effect of microbubbles on the streamwise component of velocity and vortex fluctuation intensity is somewhat similar. Compared with the single liquid phase, for the bubbly upflow, the streamwise component of vortex fluctuation intensity almost keeps unchanged in the region of $0<y^+<5$, and it increases in the region of $5<y^+<35$ and decreases in the region of $35<y^+<150$. For the bubbly downflow,

however, it also almost keeps unchanged in the region of 0<y+<5, slightly decreases in the region of 5<y+<35 and increases in the region of 35<y+<150. It can be also seen from Figs 3 and 4 that the effect of microbubbles on the spanwise component of velocity and vortex fluctuation intensity is totally different. For the bubbly upflow, the spanwise component of vortex fluctuation intensity somewhat increases near the wall and slightly decreases in the region away from the wall. However, the opposite things happen to the spanwise component for the bubbly downflow. As described above, for the bubbly upflow, when the microbubbles move towards the channel wall, they will prevent the high–frequency and small–scale spanwise vortexes in the buffer layer from developing towards the channel centre. And the microbubble accumulation near the channel wall may weaken energy transfer and scale transformation between the small–scale vortexes near the channel wall and the big–scale ones in the channel centre. However, for the bubbly downflow, the microbubbles leave the wall to the channel centre, meanwhile, they will drive the high–frequency and small–scale spanwise vortexes in the buffer layer to develop towards the channel centre. That fact will enhance the energy transfer and scale transformation between the small–scale vortexes near the channel wall and the big–scale ones in the channel centre. Furthermore, for the bubbly upflow, the addition of microbubbles reduces the energy transfer from the large–scale eddies (denoting the mean flow) to the small–scale eddies (denoting energy dissipation) so the liquid–phase turbulence fluctuation decreases but the mean streamwise velocity increases. However, for the bubbly downflow, it enhances the energy transfer between both of them so the liquid–phase turbulence fluctuation increases but the mean streamwise velocity decreases.

Figure 6 shows the instantaneous spanwise vortex contour. It can be seen from Fig. 6 that the positive and negative spanwise vortexes occur in turn near the channel wall. Compared with the single liquid phase, the spanwise vortex seems to be relatively denser and stronger near the wall for the bubbly upflow, however, it seems to be relatively diluter and weaker near the wall and develops more obviously outwards for the bubbly downflow. Those phenomena are in agreement with the above inferences.

The effect of microbubbles on velocity fluctuation intensity of the liquid phase will cause the change of Reynolds shear stress, as shown in Fig. 7. Compared with the single liquid phase, for the bubbly upflow, the liquid–phase Reynolds shear stress decreases in the region away from the channel wall; however, for the bubbly downflow, the Reynolds shear stress increases in the wide region of the channel centre and decreases in the region near the buffer layer. The liquid–phase Reynolds shear stress modulated by microbubbles is relatively complicated, and it is related to changes of intensity and frequency of the turbulence bursting events (i.e., the turbulent vortex near the wall), as analyzed above. As we all know, the function of Reynolds shear stress is to extract energy from the mean flow for the dissipation of the velocity fluctuation. For the bubbly upflow, the decrease of the liquid–phase Reynolds shear stress means that the energy transferred from the mean flow to the velocity fluctuation reduces, and thus the liquid–phase turbulence becomes weak but the mean velocity increases. Contrarily, for the bubbly downflow, the increase of the liquid–phase Reynolds shear stress in the wide region of the channel denotes that the energy transferred from the mean flow to the velocity fluctuation increases so the liquid–phase turbulence enhances but the mean velocity decreases.

Figure 8 shows the budget of Reynolds shear stress. For the bubbly upflow, the production and dissipation terms of Reynold shear stress increase in the region near the

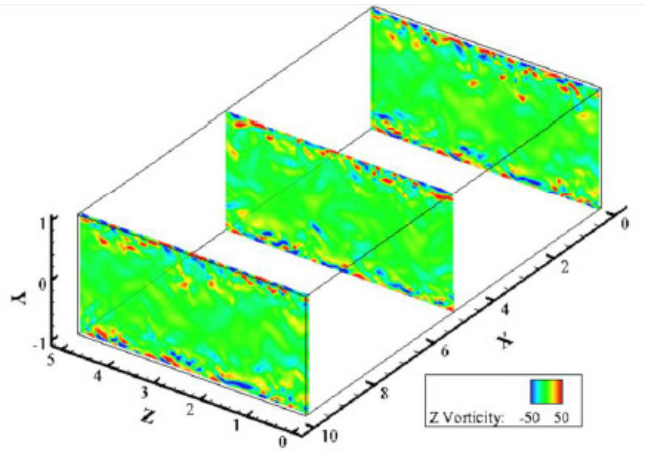


(a) Liquid phase of bubbly upflow.

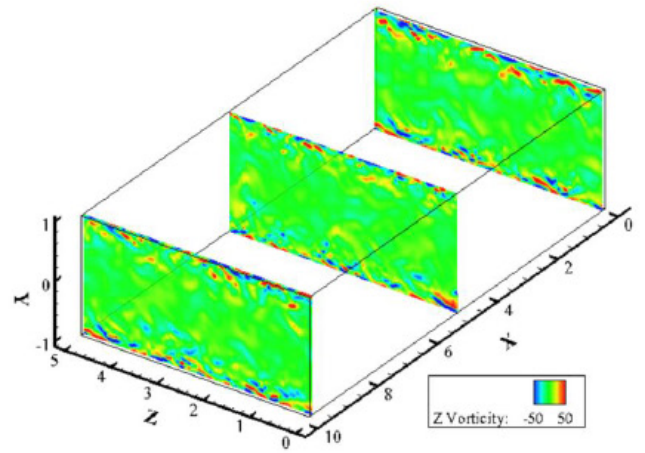


(b) Single liquid phase

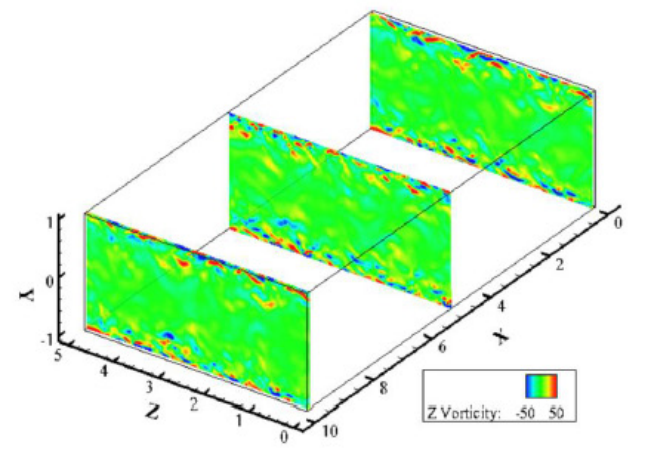


(c) Liquid phase of bubbly downflow

Figure 6: Instantaneous spanwise vorticity distribution.

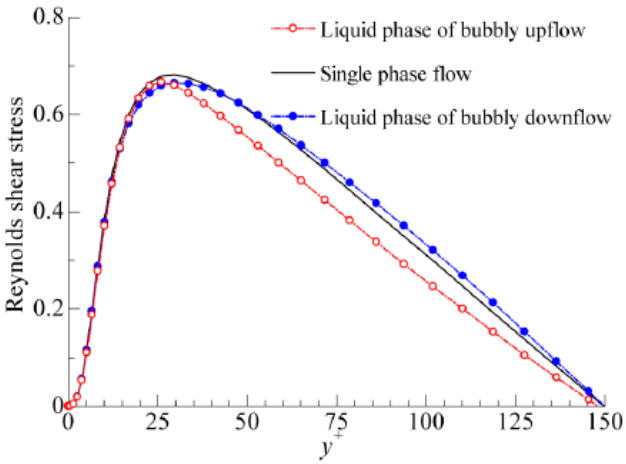


Figure 7:Reynolds shear stress profile of liquid.

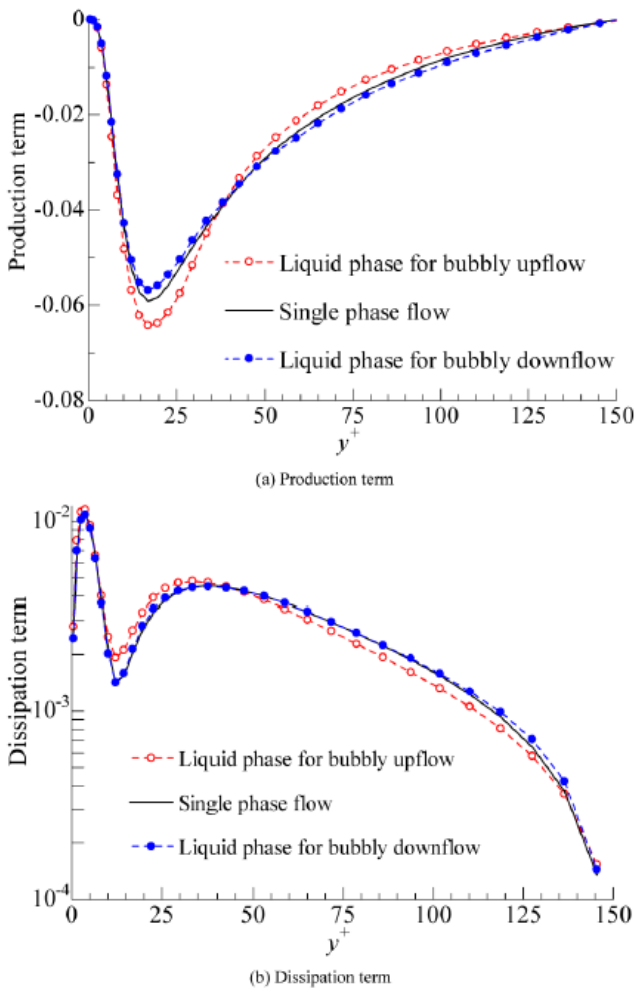


Figure 8:Budget of Reynolds shear stress.

buffer layer, and they decrease in the wide region of the channel centre compared with the single liquid phase. For the bubbly downflow, however, the effect of microbubbles on the

production and dissipation seems to be different. Namely, the production term decreases in the region near the buffer layer but increases in the wide region of the channel center, however, the dissipation term seems to decrease in the region excluding one near the wall. Additionally, it can be seen from Figs. 3 and 8 that the effect of microbubbles on the production and dissipation terms are similar to that on the streamwise component of velocity fluctuation intensity for two kinds of flow. For the present investigation, it seems to be that the streamwise component of velocity fluctuation intensity has the direct influence on the turbulence production and dissipation of Reynolds shear stress. Namely, the changed streamwise component of the liquid–phase velocity fluctuation intensity directly causes changes of Reynolds shear stress and energy transfer between the mean and fluctuation fields.

## 4. CONCLUSION

For the vertical channel bubbly flow laden with microbubbles, the influence of the flow direction on the phase distribution and the liquid–phase turbulence modulation was investigated in detail with the numerical method. The present studies show that, for different flow directions, the phase distribution pattern and the liquid-phase turbulence modulation by microbubbles are completely different. Some important conclusions can be summarized as following:

- The flow direction has the direct influence on the direction of the shear lift force, so microbubbles show different distribution pattern for the upward and downward bubbly flow; for the upward flow, the microbubbles move towards the channel and show roughly the double–peaked distribution pattern; for the downward flow, however, the microbubbles are away from the channel wall and display approximately the off–center–peaked distribution pattern.
- Different flow direction results in different motion direction of microbubbles in the wall–normal direction, so microbubbles causes different influence on the liquid–phase turbulence for the bubbly upflow and downflow; for the bubbly upflow, the liquid–phase turbulence is suppressed but the mean velocity increases; for the bubbly downflow, however, the liquid–phase turbulence is enhanced but the mean velocity decreases.
- For the present investigation, the modulation of microbubbles on the liquid–phase turbulence may be caused by the fact that the addition of microbubbles hinders (or promotes) the momentum transfer of the liquid phase between the high– and low–velocity regions.

## ACKNOWLEDGEMENT

We gratefully acknowledge the financial support from the NSFC Fund (No. 51376026). We are also grateful to the editors and reviewers for good suggestions.

## REFERENCES:

[1] Giusti, A., Lucci, F., Soldati, A., 2005. Influence of the lift force in direct numerical simulation of upward/downward turbulent channel flow laden with surfactant contaminated microbubbles. Chem. Eng. Sci. 60(22), 6176–6187

[2] Hibiki, T., Goda, H., Kim, S., Ishii, M., Uhle, J., 2004. Structure of vertical downward bubbly flow. Int. J. Heat Mass Transfer 47(8–9), 1847–1862

[3] Kashinsky, O.N., Lobanov, P.D., Pakhomov, M.A., Randin, V.V., Terekhov, V.I., 2006. Experimental and numerical study of downward bubbly flow in a pipe. Int. J. Heat Mass Transfer 49, 3717–3727

[4] Kashinsky, O.N., Randin, V.V., 1999. Downward bubbly gas–liquid flow in a vertical pipe. Int. J. Multiphase Flow 25(1), 109–138

[5] Laín, S., Bröder, D., Sommerfeld, M., 2002. Modeling hydrodynamics and turbulence in a bubble column using the Euler–Lagrange procedure. Int. J. Multiphase Flow 28, 1381–1407.

[6] Legendre, D., Colin, C., Fabre, J., Magnaudet, J., 1999. Influence of gravity upon the bubble distribution in a turbulent pipe flow: Comparison between numerical simulations and experimental data. J. Chim. Phys. 96(6), 951–957

[7] Legendre, D., Magnaudet, J., 1998. The lift force on a spherical bubble in a viscous linear shear flow. J. Fluid Mech. 369, 81–126.

[8] Lelouvetel, J., Nakagawa, M., Sato, Y., Hishida, K. 2011. Effect of bubbles on turbulent kinetic energy transport in downward flow measured by time–resolved PTV. Exp. Fluids 50, 813–823.

[9] Lelouvetel, J., Tanaka, T., Sato, Y., Hishida, K., 2014. Transport mechanisms of the turbulent energy

[10] cascade in upward/downward bubbly flows. J. Fluid Mech. 2014, 741, 514–542.

[11] Lu, J.C., Tryggvason, G., 2006. Numerical study of turbulent bubbly downflows in a vertical channel. Phys. Fluid. 18, 103302

[12] Lu, J.C., Tryggvason, G., 2007. Effect of bubble size in turbulent bubbly downflow in a vertical channel. Chem. Eng. Sci. 62(11), 3008–3018

[13] Ortiz–Villafuerte, J., Hassan, Y., 2006. Investigation of microbubble boundary layer using particle tracking velocimetry. J. Fluid Eng–T ASME 128(3), 507–519.

[14] Pang, M.J., Wei, J.J., Yu, B., 2010. Numerical study of bubbly upflows in a vertical channel using the Euler–Lagrange two–way model. Chem. Eng. Sci. 65, 6215–6228

[15] Pang, M.J., Wei, J.J., Yu, B., 2011. Study on dependence of hydrodynamic characteristics on gravity in a vertical upward channel bubbly flow. Adv. Space Res. 48, 1392–1402

[16] Sun, X., Paranjare, S., Ishii, M., Uhle, J.,2004. LDA measurement in air–water downward flow. Exp. Therm. Fluid Sci. 28, 317–328

[17] Terekhov, V.I., Pakhomov, M.A., 2008. The Effect of bubbles on the structure of flow and the friction in downward turbulent gas–liquid flow. High Temperature, 46(6), 854–860.